J Mater Sci: Mater Electron (2017) 28:15246–15251
DOI 10.1007/s10854-017-7403-7

Intragranular defects and Abrikosov–Josephson vortices in Bi-2223 bulk superconductors

M. Hernández-Wolpez[1] · A. Cruz-García[2] · R. F. Jardim[3] · P. Muné[2]

Received: 3 April 2017 / Accepted: 23 June 2017 / Published online: 30 June 2017

Abstract The Abrikosov–Josephson (AJ) vortices that emerge at intragranular defects of Bi-2223 bulk superconductors are detected. The study is based on the combination of magnetic and transport characterizations with a brief theoretical formulation that allow estimating the minimum angle of the intragranular planar defects where the AJ vortices emerges for a given applied magnetic field. Measurements of magnetization versus applied magnetic field, $M(H_a)$, in powder samples reveal that the intrinsic anisotropy effects of the grains in these materials suffer almost a complete attenuation due to their high shape anisotropy. In fact, powder samples behave as composed of isotropic grains with lower critical field ~80 Oe. However, a more detailed analysis of the quasi-linear part of these curves show that the penetration of the magnetic flux into intragranular defects occurs at similar values of applied magnetic fields than those reported in whiskers or well textured ceramics for their two main perpendicular directions which are lower values than ~80 Oe. Finally, taking into account a brief theoretical formulation, we have found that in the case of defects where the magnetic flux penetrates perpendicular to the *c*-axis of the crystallites (~30 Oe) approximately the stacking faults and defects with misorientation angles higher than ~14° can be the main causes of flux-trapping, but the mechanism may change to low misorientation angles defects, less than ~6°, when the intergranular magnetic field is approximately parallel to the *c*-axis (~60 Oe).

1 Introduction

The Bi-2223 superconductors are promising materials for reducing energy consumption in practical applications, such as magnets, motors, current leads, power cables [1–3] and fault current limiters [1, 4]. The grains in Bi-2223 superconductors have a complex structure due to their high intrinsic anisotropy [5, 6] and a network of planar defects [5, 7, 8]. These defects, such as stacking faults [9] or colonies of low angle boundaries, greatly affect the determination of the lower critical field of the grains, H_{c1g}, that is defined as the magnetic field starting from which the magnetic flux penetrates into the grains. As a consequence of their high shape anisotropy, the demagnetizing factors along the main directions of the grain are quite different [10]. In samples with low connection among the grains, i.e. low critical current density, the effects of the demagnetizing factor at the level of the sample can be disregarded. Such a approximation is even better for powder samples. Under these conditions, the grain's properties mainly determine the magnetic flux penetration and its trapping in polycrystalline superconductors.

Despite the complex structure of the polycrystalline Bi-2223 superconductors mentioned above, several measurements of magnetization as a function of applied magnetic field in powder samples, $M(H_a)$, shows a Bean-like behaviour [11]. Apparently, the powder samples behave as aggregates of isotropic grains free of defects and lower critical field ~80 Oe at 77 K. This conclusion is based on the deviation of the quasi-linear behaviour observed in the $M(H_a)$ curve and its later saturation for applied magnetic

✉ P. Muné
mune@uo.edu.cu

[1] Departamento de Física Universidad de Camagüey,Ctra, Circunvalación Norte, Km 5 1/2, Camagüey, Cuba

[2] Departamento de Física, Universidad de Oriente, Patricio Lumumba s/n, P. O. Box 90500, Santiago de Cuba, Cuba

[3] Instituto de Física, Universidade de São Paulo, CP 66318, São Paulo, SP 05315-970, Brazil

fields ~300 Oe. The causes of such a behaviour should to be clarified. Moreover, the intrinsic anisotropy of the superconductor materials should provoke a dependence of the intragranular lower critical fields, H_{c1}, with respect to the angle between the magnetic field and the main axis of the grains (c-axis) [10]. It should manifest as double step behavior in the $M(H_a)$ curve, but as was mentioned it is not experimentally observed.

On the other hand, the existence of three types of vortices inside of the type II superconductors have been reported elsewhere [12]. The Abrikosov vortices (A), the Josephson vortices (J) and the Abrikosov–Josephson vortices [13] which are located in the intragranular region free of defects, in the high angle boundaries and in the planar defects [14], respectively. Gurevich has calculated the lower critical field of the planar defects [12], H_{c1d}, but the authors have not found in the literature the application of this result to experimental data in the case of polycrystalline samples. However, it could be the explanation of the wide range of H_{c1} reported for different types of Bi-2223 superconductors. It has been reported that H_{c1} perpendicular to the c-axis is very low and close to 8 Oe at 77 K in Bi-2223/Ag tapes [15] and has been estimated that $H_{c1} \sim$ 60 Oe at the same temperature along the c-axis in Bi-2223 whiskers [16]. Those values of H_{c1} may correspond to the lower intergranular and/or intragranular defects critical field, since they belong to the first deviation from the linear behaviour observed in the $M(H_a)$ curve obtained in polycrystalline specimens. We also mention that Job and Rosenberg [17], following a similar procedure for determining H_{c1}, have found a value of ~30 Oe in ceramic samples at 77 K. They considered this value as an estimate for the case when the magnetic field is applied parallel to the a–b plane, which is a factor of 5 or 6 times smaller than the case when the magnetic field is applied parallel to the c-axis, being a result consistent with the strong anisotropy of these Bi-2223 materials.

In a previous paper we have demonstrated that in the interval of applied magnetic fields of ($30 \leq H_a \leq 80$) Oe, the penetration and trapping of the magnetic flux occur mainly into intragranular defects [18].

In the present work, we have combined magnetic and transport characterizations with a brief theoretical formulation that allows estimating the minimum value of planar defect angles where the AJ vortices emerge. First, we demonstrate that the intrinsic anisotropy of the grains may be compensated by their shape anisotropy. After that, by using a brief theoretical formulation, we estimate the minimum misorientation angle of the intragranular planar defects where the AJ vortices emerge for a given applied magnetic field. Finally, we show the planar defect angles that correspond to lower critical fields reported for whiskers [16] and textured ceramics [17] which are related with the two main direction of the grains. Our experiments and calculations allow evaluating the intragranular structure of defects in powder and pellet samples of Bi-2223 superconductors.

2 Experimental procedure

$Bi_{1.65}Pb_{0.35}Sr_2Ca_{2+x}Cu_{3+x}O_y$ samples with $x = 0.2$ (**D1**) and 0.5 (**D2**), respectively, were obtained by solid state reaction method as described elsewhere [18].

Magnetization as a function of low applied magnetic fields $M(H_a)$, were measured by using a commercial Quantum Design SQUID magnetometer. In these experiments, powders of a given sample were cooled in zero applied magnetic field from room temperature down to 77 K. After this step, the applied magnetic field H_a was then increased from 0 to 500 Oe, in steps of 5 Oe and the magnetization was measured for each value of H_a.

Measurements of $J_c(0, H_{am})$ were performed using the standard dc four-probe method in pellet samples with typical dimensions of d = 0.5 mm (thickness), w = 2 mm (width), and l = 10 mm (length). This type of measurement corresponds to the so-called *flux trapping curves*, as described elsewhere [19]. The samples are cooled down to 77 K in zero applied magnetic field, similarly to the described above. Then, a certain value of magnetic field H_{am} is applied to the sample for approximately 30 s, reduced to zero, and the critical current density is determined by using the criterion of 1 μV. Finally, the sample is warmed up to temperatures higher than the superconducting critical temperature and cooled down to 77 K in zero applied magnetic field. By repeating these steps for different values of H_{am}, the *flux trapping curve* is obtained. The values of the critical current density in the samples were ~100 A/cm^2.

3 Results and discussion

3.1 Magnetic characterization

In Fig.1 the $M(H_a)$ curves for two samples are shown. These curves exhibit a quasi-linear behavior in the interval $0 < H_a < 80$ Oe apparently related to the Meissner state of the grains of the powder samples. Both curves display also a Bean-like behaviour [11] in the whole range of applied magnetic field $0 < H_a < 500$ Oe.

In order to clarify these results, we must take into account some aspects regarding the grain's superconducting properties in Bi-2223 ceramic samples. These are useful to define H_{c1d} properly. The anisotropic behaviour of cuprate oxides is characterized by two different lower critical fields when the magnetic field is applied parallel and

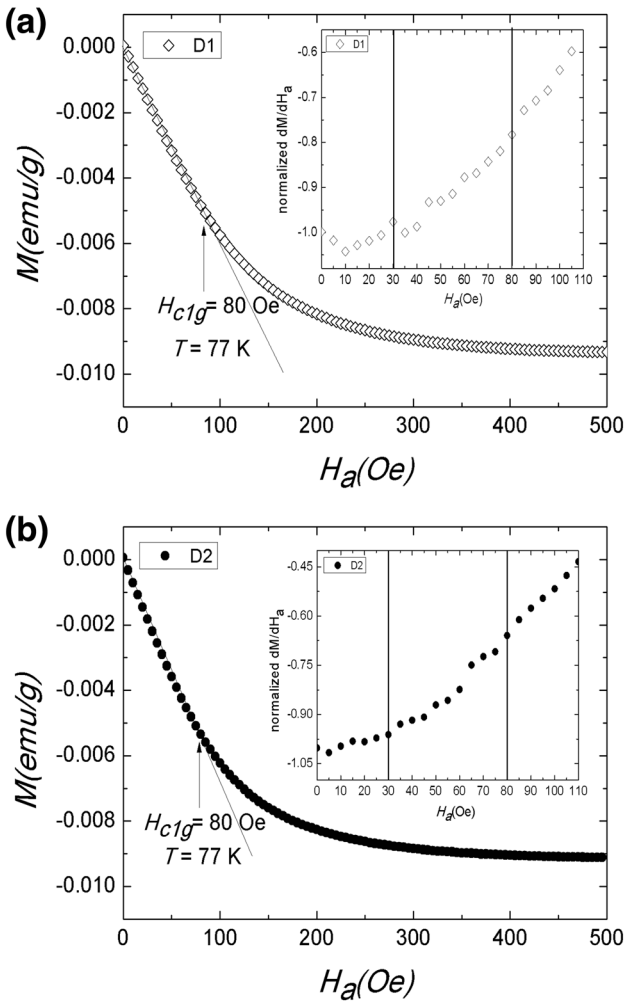

Fig. 1 Magnetization as a function of applied magnetic field in the powder samples: **a** sample **D1** and **b** sample **D2**. In both panels the *insets* show a normalized $dM(H_a)/dH_a$ as a function of applied magnetic field in the interval $0 < H_a < 110$ Oe of the powder samples **D1** and **D2**, respectively

perpendicular to the *c*-axis of the grains, respectively: $H_{c1g\|c}$ and $H_{c1g\perp c}$ [10]. Due to the high anisotropy of these materials a two-step behaviour should be observed in the $M(H_a)$ dependence. However, previous results have shown that the powder samples of Bi-2223 behave as made up of isotropic grains with lower critical field ~80 Oe [18, 20, 21]. A possible explanation of such a behaviour is the total or partial compensation of the intrinsic anisotropy by that related to the grain's shape that is platelet-like for the Bi-2223 phase [22]. Hence, the grains can be simulated as isotropic ones with lower critical field ~80 Oe and demagnetizing factor zero. Mathematically speaking, one has $(1 - G_{\perp c})H_{c1g\|c} = (1 - G_{\|c})H_{c1g\perp c} = 80$ Oe. Here, $G_{\perp c}$ and $G_{\|c}$ represent the demagnetizing factors when the intergranular magnetic field is perpendicular and parallel to the *c*-axis of the grains, respectively. If we consider the

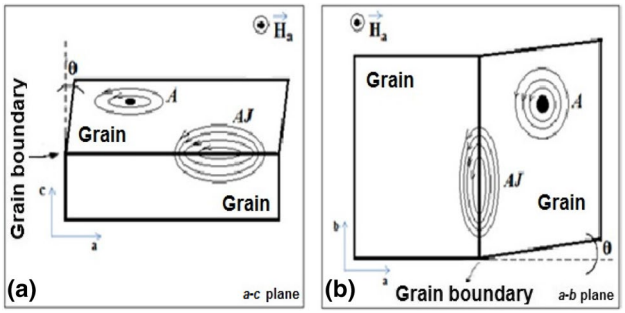

Fig. 2 Hypothetical sketch of two vortices which may be related with the different values of H_{c1} reported in the literature. In the case of the AJ vortices only the anisotropic core is represented in a magnified way. In the case of the A vortices, the normal core and the circulating currents are represented by a *dark circles* and *circular* or *elliptic lines*, respectively

grains as oblate (planetary) shperoids, $G_{\perp c} = 0.0696$ and $G_{\|c} = 0.861$ [23] if L_a/L_c is taken ~10 [18, 20]. Such values of the demagnetizing factors may compensate the effects of the intrinsic anisotropy if it is 5–6 times for the lower critical fields as reported elsewhere [17]. Thus, the grains can be regarded as isotropic ones, with lower critical field ~80 Oe and demagnetizing factor zero in a first approximation. Nevertheless, a detailed study of the quasi-linear behaviour for the interval $0 < H_a < 80$ Oe has shown that the penetration and trapping of the magnetic flux in this region is essentially intragranula [18].

3.2 Main types of Abrikosov and Abrikosov–Josephson vortices

In Ref. [18] a detailed explanation about the stepped behaviour of the $J_c(0, H_{am})$, dM/dH_a (see Fig. 1 and M/H_a versus H_a curves in the interval of applied magnetic fields, $(30 \leq H_a \leq 80)$ Oe was given. However, in order to explain the nature of the flux, which emerges at the intragranular, we show in Fig. 2 the hypothetical sketch of two vortices that we will be used to explain the behaviour of the samples that it shows at the Figs. 1 and 3.

Notice that the core of AJ vortices are always anisotropic, since the intragranular planar defects impost such a condition. However, in the A vortices, both cores and circulating currents, may be isotropic or anisotropic depending on the plane where the currents are circulating. Nevertheless, we may avoid such complication by means of a shift of variable as described elsewhere [24]. Thus, all the calculations are valid if one changes λ by $\sqrt{\lambda_{ab}\lambda_c}$ and ξ by $\sqrt{\xi_{ab}\xi_c}$, where the subscripts represent the different components of the tensor in each case. Within this context, all the Abrikosov (A) vortices can be treated as isotropic ones and the (AJ) vortices represented by two (A) isotropic vortices images in both sides of the planar defects [2, 25].

As we will show in the following subsection, the angle of the planar defect in which a AJ vortex may emerge is a function of the applied magnetic field and the effective $\kappa = \sqrt{\lambda_{ab}\lambda_c}/\sqrt{\xi_{ab}\xi_c}$, which varies from the one type of vortex to the other. This paper chiefly deals with the defects related with the misoroientation angles between the axes of the crystallites that conform the defect. However, the effects of the stacking faults also have and important role in the trapping and penetration of the magnetic flux.

Finally, the orientation of the crystallites in the intergranular applied magnetic field changes the conditions for the penetration of the magnetic flux as has been reported elsewhere [10]. In a powder sample infinite different orientations to those shown in Fig.2 may be present. Fortunately, the dependence of the lower critical field of the crystallites with its orientation in the intergranular magnetic field is well known [10].

3.2.1 *Lower critical field of the planar defects as a function of the misorientation angle*

Let us express the maximum applied magnetic field, H_{am}, or the applied magnetic field, H_a, as a function of the misorientation angle of the planar defects that under these conditions are penetrated. To achieve such a objective, we based on reference [12], where the lower critical fields for Abrikosov (A) and Abrikosov–Josephson (AJ) vortices are given by the Eqs. (1) and (2), respectively:

$$H_{c1g} = \frac{\phi_0[\ln(\frac{\lambda}{\xi}) + \gamma_1]}{4\pi\mu_0\lambda^2}, \tag{1}$$

$$H_{c1d} = \frac{\phi_0[\ln(\frac{\lambda}{l}) + \gamma_2]}{4\pi\mu_0\lambda^2}, \tag{2}$$

where ϕ_0, l, λ, ξ, γ_1, γ_2 and μ_0 are the flux quantum, the core size of the AJ vortices, the London penetration depth, the coherence length, 0.497, 0.423 and the permeability of the vacuum, respectively. Note that the AJ vortices correspond to those that arise in the planar defects. Dividing Eq. (2) by Eq. (1), substituting $l = \lambda_J^2/\lambda$, $a = H_{c1d}/H_{c1g}$, $\kappa = \lambda/\xi$, and taking $b = [a\ln(\kappa) + a\gamma_1 - \gamma_2]/2$, we obtain

$$\lambda_J = \frac{\lambda}{\exp b}, \tag{3}$$

where λ_J is the Josephson penetration depth. In order to calculate the angle of the intragranular planar defect as a function of a, we assume a relationship among the critical current density across the planar defect, J_s, the depairing current density, J_d, and $\theta_0 = 5°$, as given elsewhere [26]

$$J_s = J_d \exp\left(-\frac{\theta}{\theta_0}\right). \tag{4}$$

In Eq. (4), the pre-exponent of the current density has been taken as the depairing current density of the grains. Here, we have considered two important features of polycrystalline Bi-2223 samples: the small thickness of the platelet grains, which is typically ~100 nm, and there are defects inside the grains, for that reason the thickness of the large Josephson junctions could be even smaller. These considerations support that the thickness of the junctions, are smaller than λ and consequently justify the use of J_d in Eq. (4) [27].

Taking into account that $l=\lambda_J^2/\lambda = 3\sqrt{3}J_d\xi/4J_s$ (Ref. [12]) one obtains

$$\theta = -\theta_0\left[\ln\left(\frac{3\sqrt{3}}{4\kappa}\right) + a\ln\kappa + a\gamma_1 - \gamma_2\right]. \tag{5}$$

As a is H_{c1d} normalized to the H_{c1g}, then we have obtained the desired function. By using Eq. (5) properly, values of H_{am} or H_a can be converted to angles using $\kappa = 83$ [15].

Simple calculations reveal that a variation of ± 1 Oe in H_{am} or H_a implies a variation of ~ 0.3° in θ. Such a variation represents a relative error of 6 % in an angle $\theta = 5°$, which is a quite reasonable and acceptable value.

Notice that all the calculations have been developed assuming that the vortices' currents flow in an isotropic material where the London penetration depth and the coherence length are scalars. This case corresponds to vortices with their currents circulating in the ab plane and the used value of κ was selected in accordance with it (see Fig. 2b). For vortices similar to that represented in Fig. 2a the value of κ should be calculated as explained in the previous subsection.

In Fig. 3 we show the $J_c(0, \theta_{min})$ curves and the normalized susceptibility as a function of θ_{min}, respectively. The main features of these curves are:

1. The penetration of the magnetic flux in the powder samples is observed starting from an angle $\theta_{min} \sim 14°$.
2. In the analysed range of θ_{min}, the samples vary their normalized critical current density more than 15 and 50% in the case of the normalized susceptibility, which is perfectly appreciable by the experiment.
3. Close to $\theta_{min} = 5°$ there is another change in the behaviour of both types of curves, which is more pronounced for the sample **D2**. The separation between the curves of both samples is more appreciable starting from this angle.
4. If H_{am}= 70 Oe or H_a= 70 Oe in the flux-trapping curve and normalized susceptibility versus applied magnetic field curve, respectively, it corresponds to the magnetic flux penetration in planar defects with characteristic

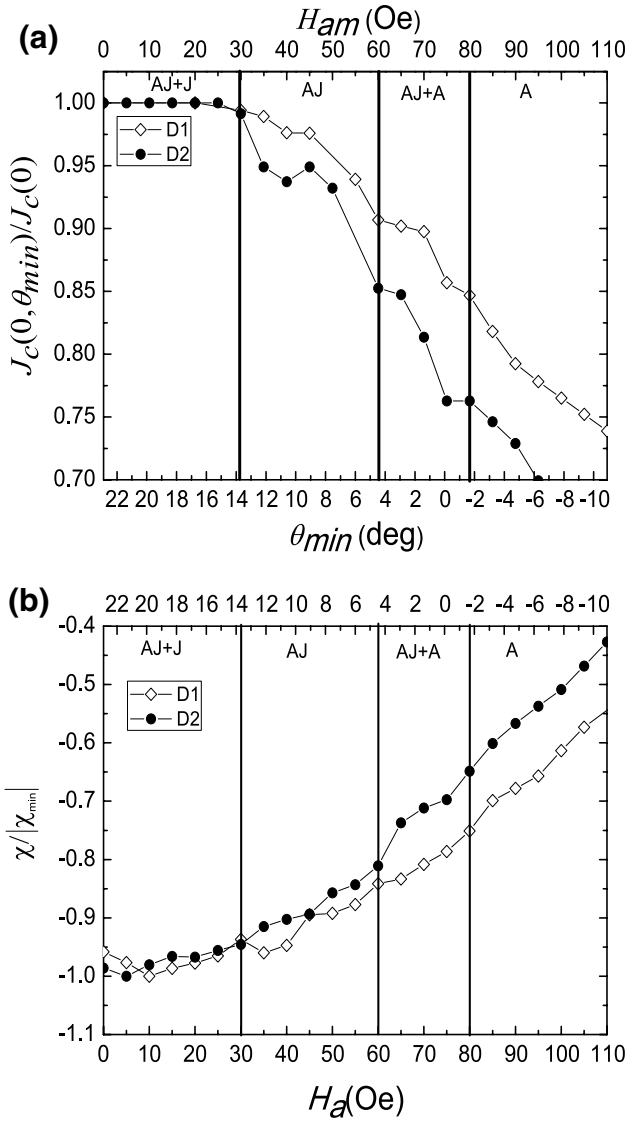

Fig. 3 **a** Normalized critical current density as a function of the θ_{min} of the samples **D1** and **D2**. **b** Normalized susceptibility as a function of θ_{min} of the powder samples **D1** and **D2**. Also in both panels we use the related magnitude in the top or bottom abscissa that correspond to H_{am} and H_a, respectively. The panels have been divided by vertical lines to show the main type of vortex that appears in each region

angle less than 2°. That magnetic flux is trapped or penetrates as A vortices in planar defects in average.

The main results obtained from the Fig. 3 are similar to the case of low angle grain boundaries in $YBa_2Cu_3O_{7-x}$ films reported elsewhere [28].

We highlight that the angle scale, which is shown in Fig. 3 changes for the case of vortices with their circulating currents in the bc and ac planes. In these cases κ increases and as a result the values of the angles that correspond to the applied magnetic fields 30 and 60 Oe also increase. If one takes $\kappa = 100$, which is also a value reported in the literature for the ab-plane [2],the results are very similar to those shown in Fig. 3. However, increasing the κ value to 500 the obtained limit angles, are 19.3° and 6.7°, respectively. Notice that the higher limit in angle increases ~6° while the lower one increases only 2°. In addition, the results at low angle are more precise, since the Eq.(2) is obtained for this type of planar defects.

The presence of stacking faults is another important issue to be considered. This type of defects have a great influence in the flux-trapping as it has been reported elsewhere [29]. For that reason and the results obtained by Job and Rosenberg [17] we assume that the stacking faults may be one of the causes of the penetration and trapping of the magnetic flux in the first step of the curves ~30 Oe as shown in Fig. 3. Moreover, if one assumes defects due to misorientation angle, in this case, the obtained value according to our calculations gives higher than 14°, which is too high to be associated with a flux creep behaviour and flux-trapping. However, the presence of other types of defects, as pores and extra-phases [18] could help the vortex pinning in those defects with higher angles [30].

On the other hand, the second step around 60 Oe corresponds to misorientation angles between 4° and 6° for both types of vortices show in Fig. 2. Those angles represent defects that may exhibit a flux creep behaviour and consequently, these may trap the magnetic flux [31].

4 Conclusions

We have carried out a systematic study of Bi-2223 superconducting samples by means of the penetration and trapping of magnetic flux at low applied magnetic field.

We have obtained that the highly anisotropic grains of these polycrystalline superconducting samples behave as isotropic ones in low applied magnetic fields because the effects of the shape anisotropy may be compensated by those provoked by the intrinsic anisotropy. It causes the almost total attenuation of the anisotropy effects in the determination of the lower critical fields. Calculations and experimental data support this explanation.

Based on this general feature of the Bi-2223 superconductors and the results obtained by Gurevich [14], we have found a correlation between the applied magnetic field and the minimum angle that characterized certain grain boundary or planar defect where the magnetic flux may penetrated. Starting from this correlation, the characteristics of the grain boundaries are linked to the penetration and the trapping. The magnetic flux is trapped for planar defects with similar angles to those reported elsewhere [28] for the $YBa_2Cu_3O_{7-x}$ films.

The main drops in the $J_c(0, H_{am})$ curves inside the stepped region are close to the values of $H_{c1\parallel c}$ and $H_{c1\perp c}$ reported in the Refs. [16] and [17], respectively.

We have found that in the case of defects where the flux penetrates approximately perpendicular to *c*-axis [17] a superposition of pinning mechanisms should be the cause of flux-trapping, but it could change to low misorientation angles defects, ~ 6°, when the intergranular magnetic field is approximately parallel to the *c*-axis [16]. The experimental evidences that are given here strongly suggest that we are detecting the transition from AJ vortices to A ones inside the grains of Bi-2223 bulk superconductors.

Our experiments allow also evaluating the effects of intragranular planar defects by means of magnetic and transport measurements. The doping with Ca and Cu from 0.2 to 0.5 in the Bi-2223 stoichiometry increases the penetration and trapping of the magnetic flux in the sample, probably due to an increase in the defects density.

Acknowledgements We would like to express our gratitude to A. Gurevich for several suggestions and the critical reading of the manuscript. We also thank E. Altshuler and E. Govea-Alcaide for useful discussions. This work was supported by the Brazil's agencies FAPESP, CNPq, and CAPES under Grant CAPES/MES No. 104/10.

References

1. J.E. Evetts, B.A. Glowacki, Supercond. Sci. Technol. **13**, 443 (2000)
2. D. Larbalestier, A. Gurevich, D.M. Feldmann, A. Polyanskii, Nature **414**, 368 (2001)
3. A. Matsumoto, H. Kitaguchi, Supercond. Sci. Technol. **27**, 015002 (2014)
4. M. Noe, M. Steurer, Supercond. Sci. Technol. **20**, R15 (2007)
5. F. Warmont, H. Jones, Supercond. Sci. Technol. **14**, 145 (2001)
6. D. Daghero, A. Masuero, P. Mazzetti, A. Stepanescu, Phys. C **341–348**, 1869 (2000)
7. K. Kishida, N.D. Browning, Phys. C **351**, 281 (2001)
8. M. Hernández-Wolpez, E. Martínez-Guerra, R.F. Jardim, P. Muné, Rev. Mex. Fis. **62**, 515 (2016)
9. F. Nakao, K. Osamura, Supercond. Sci. Technol. **18**, 513 (2005)
10. V.A. Finkel, Low Temp. Phys. **25**, 410 (1999)
11. C.P. Bean, Rev. Mod. Phys. **36**, 31 (1964)
12. A. Gurevich, Phys. Rev. B **48**, 12857 (1993)
13. A. Gurevich, L.D. Cooley, Phys. Rev. B **50**, 13563 (1994)
14. A. Gurevich, Phys. Rev. B **46**, R3187 (1992)
15. M. Majoros, L. Martini, S. Zainella, Phys. C **282**, 2205 (1997)
16. I. Matsubara, R. Funahashi, K. Ueno, H. Yamashita, T. Kawai, Phys. C **256**, 33 (1996)
17. R. Job, M. Rosenberg, Phys. C **172**, 391 (1991)
18. M. Hernández-Wolpez, A. Cruz-García, O. Vázquez-Robaina, R.F. Jardim, P. Muné, Phys. C **525–526**, 84 (2016)
19. E. Altshuler, S. García, J. Barroso, Phys. C **177**, 61 (1991)
20. P. Muné, E. Govea-Alcaide, R.F. Jardim, Phys. C **384**, 491 (2003)
21. E. Govea-Alcaide, R.F. Jardim, P. Muné, Phys. C **423**, 152 (2005)
22. Y. Kimishima, H. Ichikawa, S. Takano, T. Kuramoto, Supercond. Sci. Technol. **17**, S36 (2004)
23. B.D. Cullity, C.D. Grahan, in *Introduction to Magnetic Materials*, 2nd edn. (IEEE Press, Wiley, Hoboken, 2009)
24. T.P. Orlando, K.A. Delin, in *Foundations of the Applied Superconductivity* (Adisson-Wesley, New York, 1991)
25. F. Xue, Y. Gu, X. Gou, J. Supercond. Nov. Magn. **29**, 2711 (2016)
26. H. Hilgenkamp, J. Mannhart, Rev. Mod. Phys. **74**, 485 (2002)
27. A. Gurevich, arXiv:cond-mat/0207526v1 (2002) Accessed 23 Jan 2017
28. T. Horide, K. Matsumoto, Y. Yoshida, M. Mukaida, A. Ichinose, S. Horii, Phys. Rev. B **77**, 132502 (2008)
29. V. Kataev, N. Knauf, B. Buchner, D. Wohlleben, Phys. C **184**, 165 (1991)
30. S.I. Kim, F. Kametani, Z. Chen, A. Gurevich, D.C. Larbalestier, T. Haugan, P. Barnes, Appl. Phys. Lett. **90**, 252502 (2007)
31. J. Hasnish, A. Attenberger, B. Holzapfel, L. Shultz, Phys. Rev. B **65**, 052507 (2002)